Journal of The Electrochemical Society, **151** (10) E315-E321 (2004)
0013-4651/2004/151(10)/E315/7/$7.00 © The Electrochemical Society, Inc.

Electrochemical Surface Transfer Doping

The Mechanism Behind the Surface Conductivity of Hydrogen-Terminated Diamond

Jürgen Ristein,[z] Marc Riedel, and Lothar Ley

Institute of Technical Physics, University of Erlangen, D-91058 Erlangen, Germany

Intrinsic diamond with a bandgap of 5.4 eV exhibits a surface conductivity (SC) of the order of 10^{-5} Ω^{-1} when terminated by hydrogen. This conductivity is carried by a hole-accumulation layer close to the surface with an areal carrier concentration of about 10^{13} cm^{-2}, and it has already been utilized for a unique kind of field effect transistor [H. Kawarada, *Surf. Sci. Rep.*, **26**, 205 (1996)]. Although the microscopic doping mechanism is still under debate. Based on the results of a variety of surface-sensitive experiments we propose a new surface-transfer doping mechanism by which electron transfer from the valence band to adsorbed, hydrated ionic species at the surface creates the holes for the surface conductivity. In order to draw a complete picture of the surface conductivity concepts from surface and semiconductor physics as well as electrochemistry have to be adopted.
 [DOI: 10.1149/1.1785797]

Manuscript submitted September 24, 2003; revised manuscript received December 23, 2003. This was Paper 536 presented at the Paris, France, Meeting of the Society, April 27-May 2, 2003. Available electronically September 27, 2004.

Although the bandgap of diamond should render the intrinsic material a perfect insulator, Landstrass and Ravi have observed more than a decade ago that nominally undoped diamond exhibits a high conductance that degrades gradually upon annealing in vacuum.[1,2] For a long time this phenomenon has been considered as destructive for any kind of electronic application of diamond, and consequently was removed by surface oxidation prior to any device preparation, Kawarada showed surprisingly that the surface conductive layer could not only be tolerated but even exploited for efficient surface field effect devices.[3] This has inspired new interest in the phenomenon of surface conductivity and subsequent investigations lead to the following picture. The value of the two-dimensional conductivity is usually of the order of 10^{-6} to 10^{-4} Ω^{-1} resulting from p-type carriers with a lateral concentration in the range of 10^{12} to 10^{13} cm^{-2} and with a mobility between 10 and 100 cm^2 V^{-1} s^{-1}.[4] Both mobility and carrier concentration are only weakly temperature dependant.[4] The mobilities are not too different from those measured for B-doped diamond, and there is thus general agreement that the carriers are holes residing in a surface-near layer.[5] The depth distribution of the acceptors responsible for the holes has been discussed controversially, ranging from species at the surface[5,6] to layers extending up to 10 nm into the diamond.[4] It has even been suggested that the acceptors form a layer buried 30 nm below the surface.[7] In the limit of a quasi-two-dimensional acceptor layer at or close below the surface the observed areal density above 10^{12} cm^{-2} holes requires a band profile such that the surface Fermi level lies within a few kT of the valence band maximum (VBM) (see below).

The surface conductivity is only observed on hydrogenated diamond surfaces and disappears after dehydrogenation or oxidation of the surface. Thus it has been suggested that hydrogen is directly responsible for the hole layer by forming particular but as yet unspecified point defects within the diamond lattice that act as shallow acceptors.[4] A number of experiments which are described in the following have, however, proven that hydrogen alone is not responsible for the phenomenon of surface conductivity. An additional species usually provided by the atmosphere is necessary as well. We propose that these species are solvated ions in a thin aqueous layer on top of the diamond surface and that the doping mechanism responsible for surface conductivity is based on an electron transfer between the diamond valence band and this electrolytic wetting layer. The key experimental results that have led to this picture are described in the following.

[z] E-mail: juergen.ristein@physik.uni-erlangen.de

Reversible Annealing of the Surface Conductivity

The first key result that clearly shows the influence of atmospheric species on the surface conductivity (SC) is demonstrated in Fig. 1. A polycrystalline diamond film that had been deposited by microwave (MW)-assisted plasma chemical vapor deposition (CVD) was brought into vacuum (high vacuum, $p \sim 10^{-6}$ mbar) and the conductance of the sample was measured by two circular gold tips of diameter δ and center distance D pressed on top of the surface. It is straight forward to show that the conductance $1/R$ thus determined is related to the two-dimensional surface conductivity $\tilde{\sigma}$ by $\tilde{\sigma} = \pi/[R \cdot \ln(2D/\delta - 1)]$ in which the geometry factor $\pi/\ln(2D/\delta - 1)$ for common tip geometries ($D/\delta \sim 5...10$) is always of the order of one. In view of the large variations that can be intentionally imposed on the SC (more than six decades) and also with respect to the scatter of conductivity values measured under nominally identical conditions on different diamond samples (~one decade), we do not distinguish between conductance measured by the two-tip method and surface conductivity and use both as synonyms. In the as-prepared state (run 1) the sample shows a surface conductivity of the order of 10^{-6} Ω^{-1} typical for CVD diamond films which is only weakly temperature dependent upon annealing in vacuum up to about 240°C. After that, and depending somewhat on the rate of the heating/cooling cycle, the conductance drops and ends up six decades below the initial value after cooling down. Ramping up and down in that state (not shown in the figure) reproduces the lower branch of the cycle. Note that the temperature necessary to remove the surface conductivity is considerably lower than the desorption temperature for the hydrogen termination of the surface atoms (around 700°C),[8] so we are in all cases dealing with hydrogenated surfaces. The thermal removal of the SC is, however, fully reversible upon re-exposure of the sample to air, and the complete cycle of vacuum annealing and air exposure can be repeated arbitrarily as long as temperatures are limited to the range used in the experiment.

The results shown in Fig. 1 have in fact been qualitatively reproduced by us and others as well on surfaces of single crystals as of polycrystalline films.[9,10] Their straight forward interpretation is that something in addition to the surface hydrogen termination is needed for the SC to occur, which is removed by thermal annealing and brought back to the surface from the atmosphere. These (for the moment unspecified) adsorbates have to be capable of creating the holes inside the diamond which give rise to the SC. In that sense they act like classical acceptors in semiconductors, but sitting on the surface instead of inside the bulk lattice. The requirement for their energy levels, however, is similar; they have to provide one unoccupied orbital very close to the edge of the valence band or even below the VBM (which is possible at surfaces, not in the bulk:) to

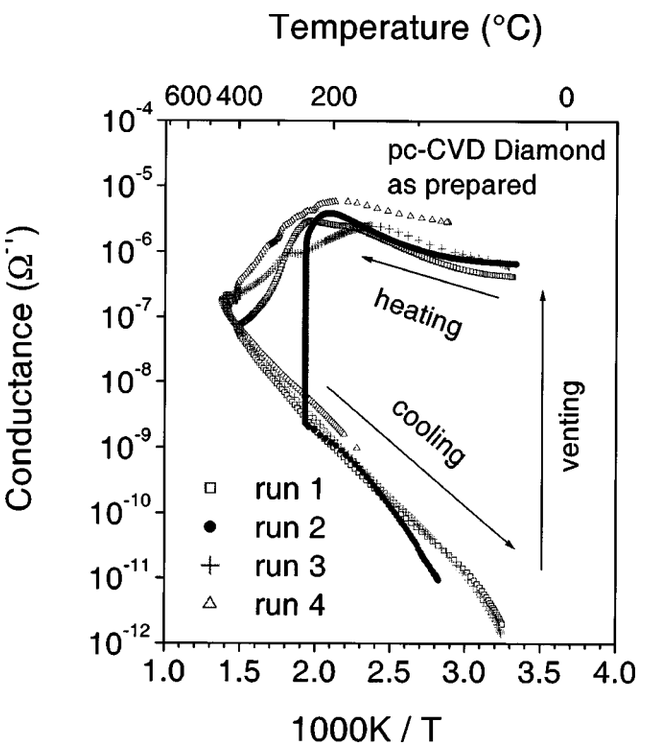

Figure 1. Response of the surface conductivity of hydrogenated diamond upon annealing in vacuum. For the second run the temperature ramp (10 K/min) was stopped at 245°C for 1 h. The decrease of the conductance at this constant temperature proves that 245°C is only an upper limit for the stability of SC in vacuum.

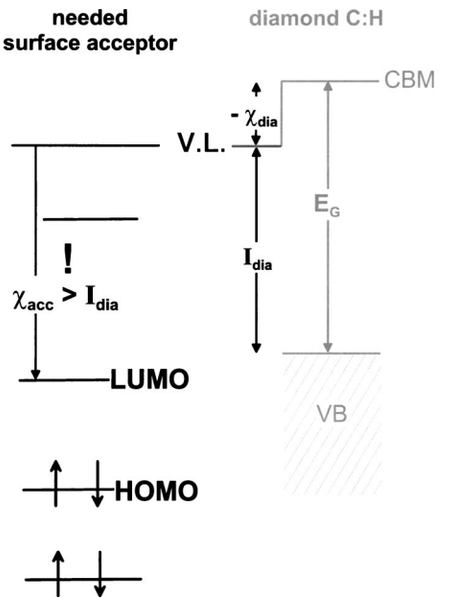

Figure 2. Level scheme of a potential molecular surface acceptor for hydrogenated diamond. Note that the electron affinity χ_{dia} has been sketched negative as determined experimentally.

accommodate and localize an electron transferred into that state from the valence band continuum. In the following chapter we discuss this electronic aspect in more detail.

The Electron Affinity of Diamond and Atmospheric Adsorbates

In order to enable an efficient electron transfer between the diamond and an atmospheric species the electronic level scheme (in the one-electron approximation) has to fulfill the criterion sketched in Fig. 2. The lowest unoccupied orbital (LUMO) of the as yet unspecified adsorbate has to be lower in energy than the highest occupied one (HOMO) of the diamond which is the valence band maximum. Since both level schemes are fixed to the vacuum level (VL) it can be equivalently stated that the electron affinity of the surface acceptor χ_{acc} has to be larger than the ionization energy I_{dia} of the diamond. The latter quantity has in fact been measured for the hydrogenated and the clean diamond (111) surface[11] as well as for the hydrogenated, the clean, and the oxygen-terminated diamond (100) surface[12] by a combination of work function measurements and photoelectron spectroscopy. As an illustration, and also to stress the large range of ionization energies and electron affinities accessible for appropriately terminated diamond, we show the corresponding results for the technologically more important (100) surface in Fig. 3. The top panel refers to an experiment where the electron affinity (left scale) and the ionization energy (right scale) have been measured accompanying the stepwise thermal dehydrogenation in ultrahigh vacuum (UHV). The data were taken at room temperature in all cases. After the initial desorption of physisorbed contaminants, a minimum ionization energy corresponding to the fully hydrogen terminated surface of 4.2 eV is found which increases to about 6.0 eV for the clean and reconstructed surface. The last data point obtained after annealing at 1200°C already reflects a partial graphitization and is no longer representative of the diamond surface. In the lower panel the same experiment for a chemically oxidized diamond (100) surface is illustrated. In this case the starting point corresponds to an ionization energy of 7.2 eV, *i.e.*, 3 eV higher than for the hydrogenated surface, and the end point of the experiment again reflects the clean and 2×1 reconstructed surface. The important number to be extracted from this experiment for the discussion of surface transfer doping is the ionization energy of 4.2 eV for the hydrogenated surface. As illustrated in Fig. 2 this sets the lower limit for any potential air borne surface acceptor.

In order to evaluate this criterion we have collected experimentally determined electron affinities of more or less abundant molecular species.[13] In fact we find only values below 2.3 eV for common atmospheric constituents, between 2.5 and 3.1 eV for the halogen molecules, and even for halogen radicals no more than 3.61 eV for chlorine as the most electronegative one. Thus, among isolated molecular or atomic species, the threshold criterion for the electron affinity of 4.2 eV is not met. Simply for energetic reasons we are therefore forced to take more complex atmospheric electronic systems as possible surface acceptors into account.

The Chemical Potential of Electrons in Atmospheric Electrolytic Systems

Referring to earlier experiments by Ri *et al.*,[6,14] who suggested hydronium ions as surface acceptors, we consider in the following the energetics of such an electron exchange mechanism in order to check its compatibility with the diamond band diagram. Within this new concept the doping mechanism does not only involve an electron transfer to an isolated molecular surface adsorbate, but is part of the following redox reaction that is driven toward an equilibrium between two a electron reservoirs, the diamond (valence band) on the one side and redox couple in an electrolytic environment on the other side

$$\text{diamond} \rightarrow \text{diamond}^{2+(\text{holes})} + 2e^- \quad [1]$$

$$2H_3O^+ + 2e^- \rightarrow H_2 + 2H_2O \quad [2]$$

We have chosen hydronium ions in equilibrium with molecular hydrogen as a very plausible but not the only possible example of a redox couple present under atmospheric conditions in the moisture layer expected on a diamond surface. Formally the diamond valence band with and without two holes plays the role of the second redox

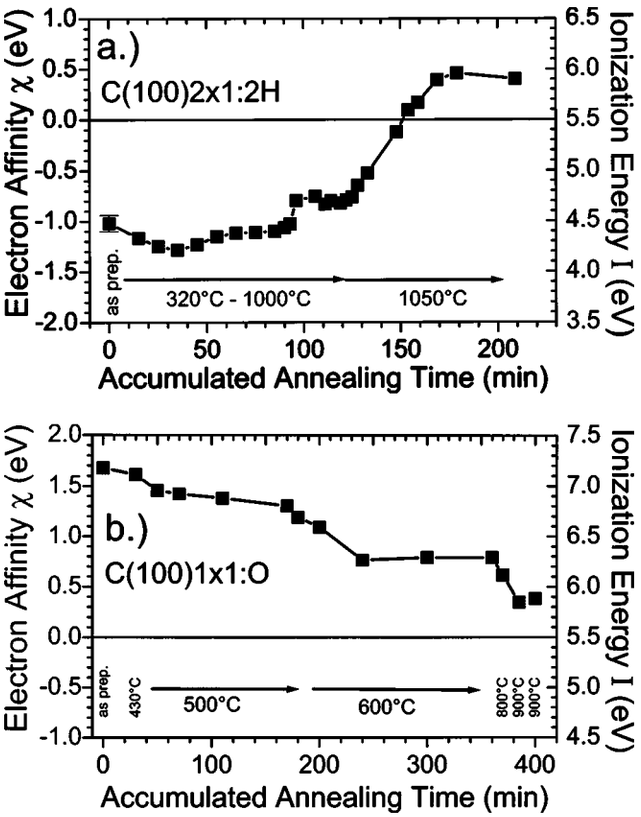

Figure 3. Electron affinity and ionization energy for the diamond (100) surface as a function of surface termination. (a) Transition from a hydrogenated to a clean surface; (b) transition between an oxygen terminated and a clean surface.

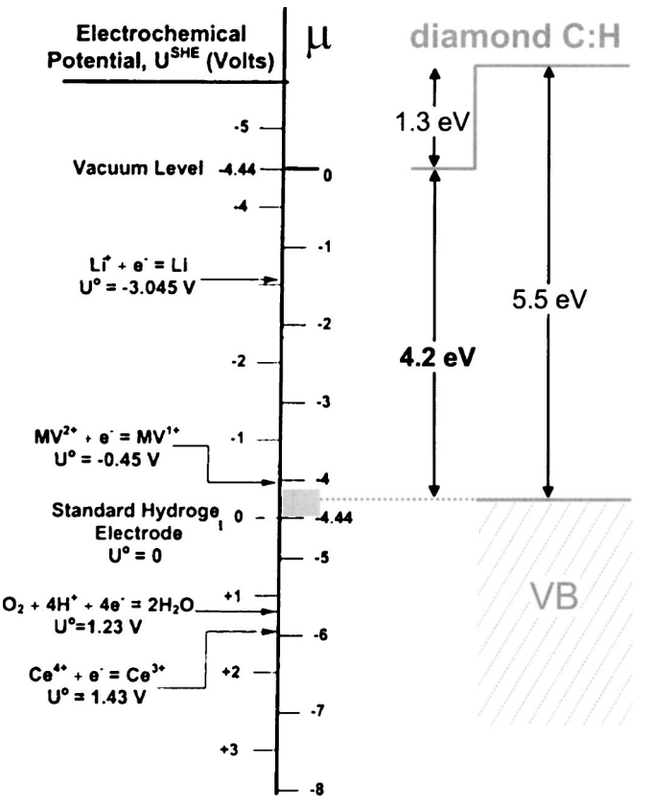

Figure 4. Alignment between the electrochemical potential scale and the vacuum level and relation to the diamond band diagram.

pair participating in the total redox reaction. In this sense the diamond is oxidized in a certain range below its surface by the transfer doping mechanism. In contrast to the classical oxidation of metals by acids, however, the result is not a formation of positive carbon ions going into solution and thus resulting in corrosion of the diamond. Instead, the positive charge corresponding to the transferred electrons remains as free holes in a near-surface range in the solid. In the chemist's language, as for any redox reaction the direction of electron transfer is determined by the electrochemical potentials of the participating redox couples, and one would derive this quantity from the conventional electrochemical standard potential scale. In the language of statistical physics one would rather compare the chemical potential for electrons in both electronic systems with one another, and relate this quantity to the vacuum level. Both potential scales refer to the same quantity. Since the electrochemical potential scale formally corresponds to a positive elementary charge both scales have, however, opposite signs. The alignment between both is given by the chemical potential of −4.44 eV of the standard hydrogen electrode relative to the vacuum level.[15,16] Corresponding to this offset we have aligned the electrochemical potential scale to the diamond band diagram in Fig. 4 using its ionization energy as discussed in the last paragraph. The potentials of the exemplary redox couples on this scale[17] refer to standard concentrations of the participating species (room temperature, 1 mole per liter for species in solution, and 1 bar partial pressure for species participating from a gas phase in equilibrium with the electrolyte). In order to obtain chemical potentials expected for nonstandard concentrations of redox couples one has to correct for the real concentrations via Nernst's equation. For a general redox couple involving N molecular species OX_i on the oxidized side, each participating with n_i particles to the reaction, M molecular species RED_i on the reduced side, each participating with m_i particles, and a total number of z electrons involved in the reaction, the equilibrium is formally represented by

$$\sum_{i=1}^{N} n_i \mathrm{OX}_i + z\mathrm{e}^- \leftrightarrow \sum_{i=1}^{M} m_i \mathrm{RED}_i \qquad [3]$$

and Nernst's equation, relating the chemical potential μ for the actual concentrations $[OX_i]$ and $[RED_i]$ to the standard potential μ_S valid for the standard concentrations $[OX_i]_S$ and $[RED_i]_S$, reads as

$$\mu = \mu_S - \frac{kT}{z} \ln\left[\frac{\Pi_{i=1}^{N}([\mathrm{OX}_i]/[\mathrm{OX}_i]_S)^{n_i}}{\Pi_{i=1}^{M}([\mathrm{RED}_i]/[\mathrm{RED}_i]_S)^{m_i}}\right] \qquad [4]$$

Note that the sign of the concentration dependent shift in Eq. 4 is opposite to the common textbook representations of Nernst's equation since we are referring to the chemical potential of negative electrons instead of the formal electrochemical potentials used in chemistry. In order to estimate a potential window for atmospheric moisture layers we have to make reasonable assumptions for the partial pressure of hydrogen in the atmosphere and the acidity of the moisture layer. For the former we allow a wide range of partial pressures between 1 nbar and 1 mbar that covers the value of 0.5 μbar given in the *CRC Handbook of Chemistry and Physics*[13] with a large tolerance. If we further adopt a slightly acidic pH value between 5 and 7 due to atmospheric CO_2, Nernst's equation,[4] applied to the hydronium redox couple, Eq. 2, yields an atmospheric window between −4.44 and −4.12 eV for the chemical potential μ that has been indicated by the shaded box in Fig. 4. The diamond VBM (at −4.2 eV) falls exactly into this window. Thus, considering the chemical potential for electrons in moisture layers under realistic atmospheric conditions shows that an electron transfer from the valence band of hydrogenated diamond to hydronium ions in the electrolytic layer is thermodynamically possible and thus a plausible

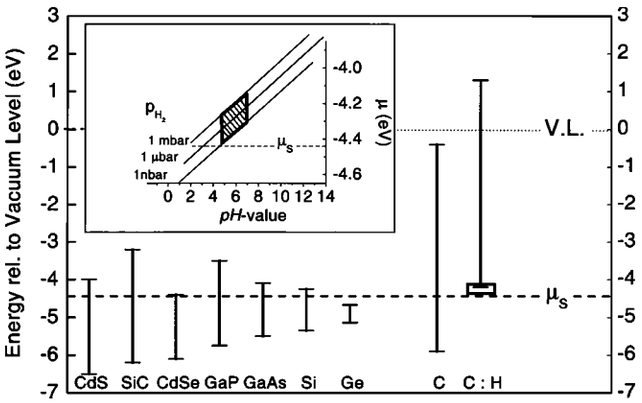

Figure 5. Comparison between the bandgaps of a number of conventional semiconductors and diamond on an absolute energy scale. The insert shows the dependence of the chemical potential of electrons in an aqueous atmospheric layer as a function of pH value and hydrogen partial pressure in atmosphere. μ_s refers to the chemical potential of the standard hydrogen electrode.

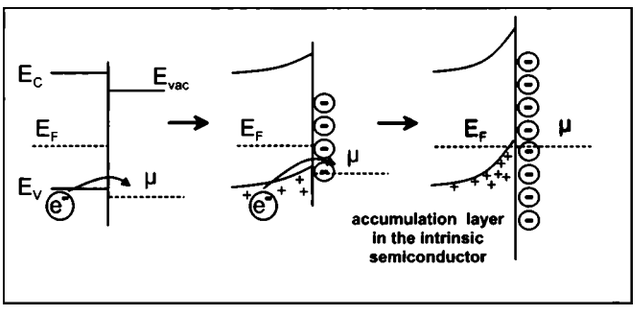

Figure 6. Evolution of a surface-near hole layer and the accompanying potential profile as a consequence of transfer doping.

microscopic mechanism for the surface transfer doping of diamond by adsorbates. The transfer of electrons from the diamond valence band into the electrolytic layer will thus proceed until finally the surface Fermi level will coincide with the chemical potential μ of the redox couple. This charge transfer is self-limiting by a simultaneous buildup of a diffusion potential as discussed in the next section.

With reference to the uncertainty of ambient conditions indicated by the atmospheric window in Fig. 4 we point out that a variation of similar size is easily encountered in the ionization energy of diamond. From our experience the cited value of 4.2 eV that is characteristic for a perfectly hydrogenated surface can sometimes easily be found some tenths of an electron volt higher, most probably due to an imperfect hydrogenation process of the surface. We also state explicitly here that estimating chemical potentials for an electron transfer reaction can in general only determine the allowed direction of the transfer. Even if allowed, such a reaction can be kinetically suppressed or only be initiated by appropriate catalysts. We return to this aspect later.

It is instructive to conclude this section on the chemical potential alignment between diamond and atmospheric electrolytes with a comparison with other semiconductors. To this end we have illustrated bandgaps with the valence and conduction bandedges for a number of common semiconductors as well as for clean and hydrogen-terminated diamond in Fig. 5 on an absolute energy scale related to the vacuum level. In the insert we have evaluated Nernst's equation for the chemical potential of electrons in the electrolyte as a function of pH value and hydrogen partial pressure in the gas phase. The typical atmospheric window discussed above is again indicated by the shaded areas in the figure and the insert. It is obvious that the valence band maximum of only diamond with a hydrogen-terminated surface overlaps the atmospheric window and thus is susceptible to an electron transfer. For all other semiconductors shown a surface-transfer doping mechanism for holes based on hydronium ions is impossible for energetic reasons. The unique role of hydrogenated diamond can thus be traced back to its rather low ionization energy of 4.2 eV compared to other semiconductors.

The Evolution of a Confined Surface-Near Hole Gas in Diamond

We explained above why atmospheric adsorbates in a moisture layer on hydrogenated diamond can be expected to extract electrons from the diamond valence band and thus act as acceptors on the surface. The role of the hydrogen termination is only indirect by lowering the ionization energy sufficiently. When a hydrogenated diamond is thus exposed to air for the first time it faces an electronic system with a chemical potential (of electrons) lower than the diamond's VBM and thus certainly lower that its own chemical potential which is the Fermi level somewhere inside the bandgap. As a result, the redox Reaction 1 is promoted, and holes are injected into the diamond and diffuse further in. Note that for every hole a compensating negative ion remains on the surface. For the hydronium ions as surface acceptors these negative ions are the acidic anions (*e.g.*, HCO_3^-), but if other redox couples are present and act as acceptors they may also be anions formed directly during the redox reaction. We present an example of such a case below. As a consequence of hole injection and diffusion a space-charge layer connected with an upward band bending potential will gradually evolve and act more and more as a barrier for further in-diffusion of holes. The transfer doping process comes to a halt when the potential profile has evolved such that the built-in potential compensates the original offset in chemical potentials, or, in other words, when the chemical potentials at the surface have equalized. We have sketched this process in Fig. 6, and now consider the band profile in the diamond after equilibration. When we define the electrostatic band bending potential $u(x)$ by the local separation between the valence band maximum $E_V(x)$ and the Fermi level, *i.e.*, $u(x) = E_V(x) - E_F$, the relation between the potential and the space-charge density $\rho(u)$ due to the holes within the diffusive tail can be expressed adopting Boltzmann statistics as

$$\rho(u) = eN_V \exp\left(\frac{u}{kT}\right) \qquad [5]$$

where e and k are the elementary charge and Boltzmann's constant, respectively, T is the temperature and $N_V = 2.7 \cdot 10^{19}$ cm^{-3} the effective valence band density of states of diamond.[18] Note that u is negative as long as the Fermi level is situated above the valence band maximum. When Eq. 5 is combined with Poisson's equation

$$\frac{d^2u}{dx^2} = \frac{e}{\varepsilon\varepsilon_0}\rho(x) \qquad [6]$$

where $\varepsilon = 5.8$ and ε_0 are the permeabilities of diamond and vacuum, respectively, a differential equation of second order results for the potential. For a semi-infinite diamond it can be solved with only the surface potential u_s as a remaining free-boundary condition. The corresponding solution and the derived profiles for the electric field and the hole density can, in fact, be expressed by simple analytic functions when they are related to appropriate units that depend on N_V and ε as intrinsic diamond properties and on the temperature: $\lambda = \sqrt{2kT\varepsilon\varepsilon_0/N_V}/e$ which amounts to 0.77 nm at room temperature for the depth scale into the diamond bulk; $2kT$ for the potential; N_V for the hole concentration $p(x)$; and $F_0 = 2kT/(\lambda e)$ which amounts to $6.5 \cdot 10^5$ V/cm at room temperature for the electric field

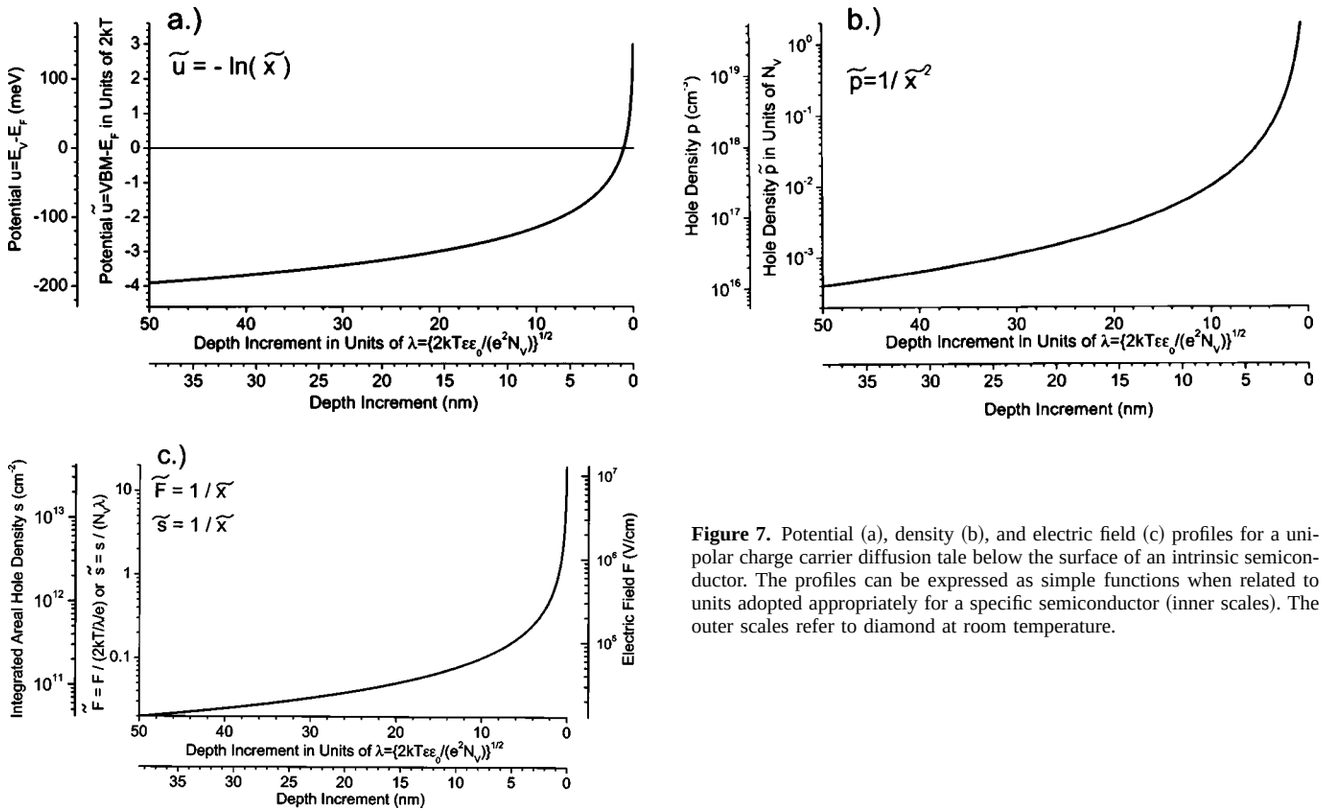

Figure 7. Potential (a), density (b), and electric field (c) profiles for a unipolar charge carrier diffusion tale below the surface of an intrinsic semiconductor. The profiles can be expressed as simple functions when related to units adopted appropriately for a specific semiconductor (inner scales). The outer scales refer to diamond at room temperature.

$F(x)$. With these adapted units the various profiles of the hole diffusion tail into the diamond can be expressed as a function of the depth scale increment $\tilde{x} = x/\lambda$ as

$$\tilde{u} = u/2kT = -\ln(\tilde{x}) \quad [7]$$

and

$$\tilde{p} = p/N_V = 1/\tilde{x}^2 \quad [8]$$

$$\tilde{F} = F/F_0 = 1/\tilde{x} \quad [9]$$

As a direct and general consequence of Poisson's equation, the electric field at a certain depth is strictly related to the total number s of holes per area integrated over the diffusive tail beyond that depth by $s(x) = \varepsilon\varepsilon_0/e \cdot F(x)$. Thus, when $N_V\lambda$ which amounts to $2.1 \cdot 10^{12}$ cm^{-2} is used as a unit for s the normalized profile $\tilde{s}(\tilde{x}) = s/(N_V\lambda)$ is also given by Eq. 9 by just replacing $\tilde{F}$ by $\tilde{s}$

$$\tilde{s} = s/(N_V\lambda) = 1/\tilde{x} \quad [10]$$

We have plotted these universal profiles which describe the unipolar charge carrier diffusion in any intrinsic semiconductor in general terms in Fig. 7. All profiles have a singularity at $\tilde{x} = 0$. This position does not refer to the semiconductor surface but instead to some position in front of the surface. The abscissa thus only represents a depth increment. The remaining boundary condition represented by the surface potential $u_s = kT \cdot \tilde{u}_s$ can now simply be implemented in the plots of Fig. 7 by choosing the position of the surface on the abscissa appropriately. Equivalently, the total number of holes per area in the diffusive tail can be chosen and Fig. 7c can be taken to determine the surface position instead of using the surface potential and Fig. 7a. For example, if the total areal hole density is known to be 10^{12} cm^{-2} the surface position on the abscissa in Fig. 7c has to be placed at 1.6 nm (2.1 λ). Transferring this surface coordinate to Fig. 7a and b as well then gives a correct description of all profiles associated with the hole layer. The larger the total areal concentration of holes induced by the surface acceptors the closer is the surface position to the singularity on the abscissa, and the steeper are the density and field profiles decaying into the bulk. For a total integrated hole concentration between 10^{12} and 10^{13} cm^{-2} as observed experimentally for the p-type layers on hydrogenated diamond the surface has to be positioned between 2.1 and 0.21 λ, respectively, as is also obtained directly from Eq. 8b. Even for the lower limit of hole concentrations usually observed 10^{12} cm^{-2} we thus find from Fig. 7c that 90% of the holes are concentrated within 15 nm below the surface (decay length from 10^{12} to 10^{11} cm^{-2}), and this range shrinks to only 1.6 nm for 10^{13} cm^{-2} holes (decay length from 10^{13} to 10^{12} cm^{-2}). From Fig. 7a or Eq. 7 one can evaluate the surface potential consistent with these hole concentrations and obtain a range between +78 and −37 meV for u_s. It is evident from these data that the Fermi level at the surface has to be situated very close to or even slightly within the valence band of the diamond in order to explain the high concentration of holes observed experimentally.

Concluding this section we may summarize as follows: as a consequence of a redox reaction of the diamond with surface acceptors in the form of an electrochemical redox couple with deep enough chemical potential, holes are induced into the diamond. They spread into the diamond but are retracted by a self-created potential. In equilibrium a diffusive tail of holes is formed with purely intrinsic properties for which the surface acceptors determine the total depth integrated density by pulling the Fermi level at the surface of the diamond to the chemical potential position of the active redox couple.

Charge Exchange Reaction Barriers and Alternative Redox Couples

The model so far presented describes the surface conductivity of diamond as a purely intrinsic phenomenon that only requires surface

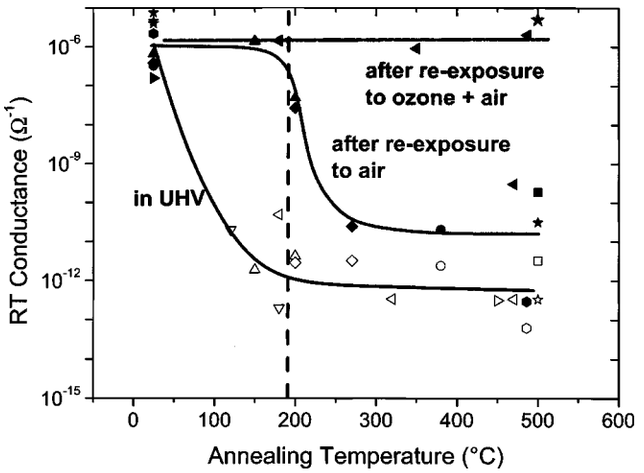

Figure 8. Response of the surface conductivity of hydrogenated diamond upon annealing in vacuum (open symbols) and subsequent exposure to air (full black symbols) and to a combination of ozone and air (light gray symbols).

hydrogen termination and the presence of an atmospheric moisture layer. The reversible removal of the surface conductivity by thermal annealing documented in Fig. 1 is interpreted by the removal of the moisture layer in vacuum or, more precisely, the desorption of the anions from the surface which can in principle happen independently from the water desorption. As long as those anions are present the hole gas is stable. (When the negative anions are removed the overall charge neutrality of the sample requires that the holes recombine in the contacts.) As long as the surface hydrogen termination of the diamond remains intact subsequent air exposure of the sample restores the surface conductivity again by the transfer doping mechanism explained above. In fact the reversible cycling of the surface conductivity should be possible as long as the annealing temperature in vacuum does not exceed the stability threshold for the hydrogen termination of about $T_{A,c} \approx 700°C$. Note that this stability threshold is dramatically reduced in air where annealing at about 200°C already leads to a loss of the surface hydrogen by oxidation and to an irreversible loss of the surface conductivity.[19] More recently we have, however, investigated the thermal removal of surface conductivity and its recovery in air in more detail, and the results are shown in Fig. 8. Each symbol in the figure corresponds to a different experiment, and altogether three different single-crystal samples with hydrogenated (100) surfaces have been used and were stepwise annealed in UHV for about 15 min. After each annealing step the conductance of the sample was measured in vacuum (open symbols), and eventually also after exposure to normal air (full black symbols). So far we have discussed only the fully reversible annealing range for which the surface conductivity always recovers to its initial value after re-exposure to air. In the experiments documented in Fig. 8 this range extends up to about 190°C (dashed line). After annealing at temperatures between 200 and 500°C the conductance recovers only marginally upon air exposure and remains below $10^{-9}\ \Omega^{-1}$ in all cases. Note that this temperature range is clearly below the desorption temperature of the surface hydrogen, and we have in fact verified in independent photo yield experiments that the surfaces were in all cases still hydrogen terminated. Nevertheless, vacuum annealing above 200°C obviously transfers diamond into a state where surface conductivity is no longer induced by atmospheric exposure in spite of an intact hydrogen termination. We are thus forced to assume that some additional ingredient is necessary for surface-transfer doping by atmospheric adsorbates. A clue about what this ingredient might be can be obtained from the filled light gray symbols in Fig. 8 which show the conductances when samples are exposed after annealing not only to air, but additionally to ozone from an ozone source. This procedure in fact restores the surface conductivity fully, and we are thus led to the conclusion that an additional conditioning, probably by oxygen radicals, is necessary for the creation of surface conductivity. It is important to note that after this conditioning samples are again in the fully reversible state, since in subsequent annealing sequences limited to 190°C the surface conductivity again fully recovers from annealing by simple air exposure without any ozone. The ozone exposure is thus only necessary for the conditioning of the surface, but is not needed afterward for the transfer doping. This amazing observation can be understood straight forwardly if we assume that ozone creates specific oxygen-related defect centers on the hydrogenated diamond surface through which the electron transfer process into atmospheric adsorbates takes place. Since the samples' surface conductivity after reconditioning by ozone can be cycled again by annealing and air exposure, the oxygen-related surface defects obviously act catalytically, *i.e.*, they reduce or allow the circumvent on of a reaction barrier for the electron exchange between diamond and adsorbates that otherwise prevents the transfer doping in spite of an appropriate alignment of the chemical potentials between them. Following this interpretation, the electrochemical transfer doping mechanism by surface adsorbates is kinetically suppressed on the perfect hydrogen-terminated surface, but activated catalytically at specific oxygen-related defects. We have illustrated this tentative model schematically in Fig. 9. The left side shows the electrons transfer across a perfectly hydrogenated surface as discussed so far, again using the hydrogen redox couple as the acceptor. In the light of our new results of Fig. 8 we are forced to conclude that the indicated transfer reaction is, in fact, kinetically suppressed. In the lower panel of the figure we have added as an example an O-H group or a bridging O atom at a surface step as two possible and plausible oxygen-related defect centers that may form during ozone conditioning of the surface. Their role in the surface transfer doping process is interpreted as providing a better overlap between the HOMO (diamond VB) and the LUMO (H_3O^+, in our case) wave functions and thus removing the kinetic hindrance of the electron transfer. Such an improvement of overlap can, in principle, be achieved by coupling of the HOMO and the LUMO to a molecular orbital of the oxygen-defect center. Following this interpretation, annealing above 200°C destroys the catalytic oxygen-related centers, *e.g.*, by converting them to dangling or weak bonds, and the reconditioning effect of the ozone treatment is due to a reformation of these centers. Note that a prolonged oxidation of the surface, *i.e.*, the replacement of the hydrogen by an oxygen termination, will raise the diamond ionization energy (Fig. 3b.) such that the alignment of chemical potentials is no longer appropriate for the surface transfer doping by atmospheric adsorbates. The expected irreversible loss of the surface conductivity is also observed in our recent experiments.[20] We must admit that the evidence for oxygen-related catalytic defects involved in the surface transfer doping mechanism is only indirect, and the tentative model suggested so far is only speculative. It would require sophisticated quantum chemical modeling to shed light on this kind of electron transfer reaction. Such calculations are in progress, and they should help to develop a complete picture of the doping mechanism behind the surface conductivity of diamond.

As a final aspect of the problem, we address the possibility of alternative redox couples instead of hydronium/hydrogen that could act as surface acceptors. This possibility was in fact suggested to the authors by Angus previously[21] and has meanwhile been elaborated somewhat further.[22] The active redox couple suggested is the hydroxyle/oxygen couple

$$2H_2O + O_2 + 4e^- \rightarrow 4\ OH^- \qquad [11]$$

that would replace Eq. 2 as acceptor redox couple. In fact the standard chemical potential of this reaction (referred to the vacuum level) is −4.84 eV, and after correction for atmospheric conditions (0.2 bar oxygen partial pressure and pH 6) via Eq. 4 a chemical potential of $\mu = -5.18$ eV results. From a purely energetic point of

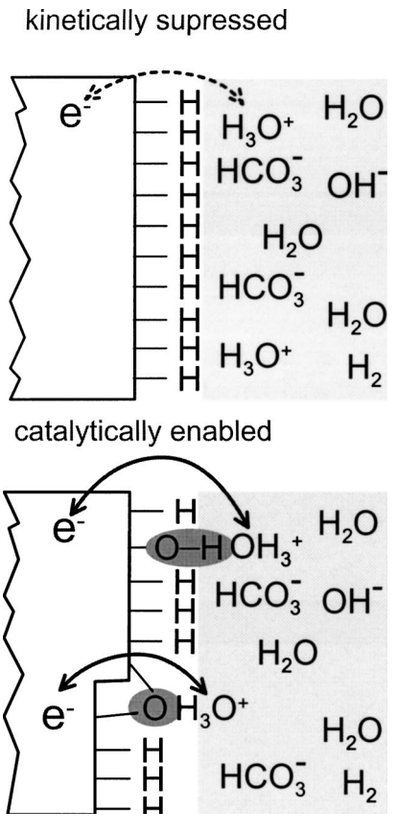

Figure 9. Tentative model for the role of catalytic oxygen-related defect centers in the surface transfer doping mechanism on hydrogenated diamond.

view this redox couple would even work as an acceptor on a diamond surface with 1 eV higher ionization energy than measured for the fully hydrogenated one.[11] In fact, Piantanida *et al.*[23] recently suggested a raise in electron affinity by about 0.8 eV as a consequence of water adsorption. This would result in an ionization energy of hydrogenated diamond in air of about 5 eV. In this scenario electrochemical surface-transfer doping would no longer work on the basis of the hydrogen redox couple, Eq. 1, but still on the oxygen redox couple, Eq. 11. One has to keep in mind, however, that the chemical potentials only suggest the possible charge exchange reactions. Those can still be kinetically suppressed by reaction barriers, *e.g.*, the necessary breaking of the molecular oxygen bond in Reaction 10 or the molecular hydrogen bond in the backwards direction of Eq. 1. (Note that for establishing equilibrium foreward and back reactions both must be possible.) The conditioning of the surfaces by ozone is apparently necessary for charge exchange, which was briefly mentioned above and will be more extensively discussed in a forthcoming paper, in fact proves the existence of some sort of reaction barrier present on the perfect hydrogenated surface unexposed to ozone. The active atmospheric redox couple is obviously suppressed by this reaction barrier, but enabled at the specific oxygen sites introduced above. If this active redox couple is in fact the hydrogen couple as sketched in the figure or the oxygen couple has yet to be determined by further experiments.

Breaking of strong molecular bonds is unnecessary for another alternative redox couple that can be expected to be active when diamond is exposed to an ozone-enriched atmosphere. If we allow for additional moisture, the experimental conditions should provide the ozone/oxygen redox couple corresponding to

$$O_3 + H_2O + 2e^- \rightarrow O_2 + 2\ OH^- \qquad [12]$$

After correcting the standard potential of this couple via Eq. 4 for the experimental conditions in our ozone experiments described above ($[O_3]/[O_2]$ approximately one, and again pH 6) we obtain a chemical potential of $\mu = -5.79$ eV for ozone in conjunction with atmospheric water as a surface acceptor. The effect of ozone in the experiments discussed above may be two-fold. On the one hand there is the reconditioning reaction by creating catalytic defect centers on the surface that was discussed above. On the other hand, during the very reaction in a humid ozone-containing atmosphere, we have the transfer doping by the very efficient redox couple, Eq. 12. We have in fact evidence that for a partially oxidized and thus less susceptible diamond surface SC can be induced in the presence of ozone (*e.g.*, following Eq. 11), but no longer by simple air exposure (*e.g.*, following Eq. 2).[20] Note that for both alternative redox couples discussed in this paragraph as surface acceptors, the anions acting on the surface of the diamond as a counter charge for the holes are provided by the hydroxyle ions created by the redox reaction itself. To conclude this section we may note that the surface-transfer doping mechanism is not limited to hydronium ions as surface acceptors, but can also be achieved by other redox couples under appropriate conditions. It appears to be a rather general phenomenon on hydrogenated diamond. It should be noted in general that the evolution of surface conductivity in atmosphere is, however, a rather slow process on the time scale of hours to days (for full evolution). Already this very obvious experimental fact indicates that substantial reaction barriers are involved in the process.

References

1. M. I. Landstrass and K. V. Ravi, *Appl. Phys. Lett.*, **55**, 975 (1989).
2. M. I. Landstrass and K. V. Ravi, *Appl. Phys. Lett.*, **55**, 1391 (1989).
3. H. Kawarada, *Surf. Sci. Rep.*, **26**, 205 (1996).
4. K. Hayashi, S. Yamanaka, H. Watanabe, T. Sekiguchi, H. Okushi, and K. Kajimura, *J. Appl. Phys.*, **81**, 744 (1997).
5. K. Tsugawa, K. Kitatani, H. Noda, A. Hokazono, K. Hirose, M. Tajima, and H. Kawarada, *Diamond Relat. Mater.*, **8**, 927 (1999).
6. S. G. Ri, K. Tashiro, S. Tanaka, T. Fujisawa, H. Kimua, T. Kurosu, and M. Iida, *Jpn. J. Appl. Phys., Part 1*, **38**, 3492 (1999).
7. A. Denisenko, A. Aleksov, A. Pribil, P. Gluche, W. Ebert, and E. Kohn, *Diamond Relat. Mater.*, **9**, 1138 (2000).
8. J. B. Cui, J. Ristein, and L. Ley, *Phys. Rev. B*, **59**, 5847 (1999).
9. M. Szameitat, X. Jiang, and W. Beyer, *Appl. Phys. Lett.*, **77**, 1554 (2000).
10. B. Koslowski, S. Strobel, and P. Ziemann, *Appl. Phys. A: Solids Surf.*, **72**, 211 (2000).
11. J. B. Cui, J. Ristein, and L. Ley, *Phys. Rev. Lett.*, **81**, 429 (1998).
12. F. Maier, J. Ristein, and L. Ley, *Phys. Rev. B*, **64**, 165411 (2001).
13. *CRC Handbook of Chemistry and Physics*, 76th ed., D. R. Lide, Editor, CRC Press, Boca Raton, FL (1996).
14. S. G. Ri, T. Mizumasa, Y. Akliba, Y. Hirose, T. Kurosu, and M. Iida, *Jpn. J. Appl. Phys., Part 1*, **34**, 5550 (1995).
15. N. Sato, *Electrochemistry at Metal and Semiconductor Electrodes*, p. 57, Elsevier, Amsterdam (1998).
16. S. Trasatti, *Pure Appl. Chem.*, **58**, 956 (1986).
17. J. C. Angus, H. B. Martin, U. Landau, Y. E. Evstefeeva, B. Miller, and N. Vinokur, *New Diamond Front. Carbon Technol.*, **9**, 175 (1999).
18. J. Kono, S. Takeyama, T. Takamasu, N. Miura, N. Fujimori, Y. Nishibayashi, T. Nakajima, and K. Tsuji, *Phys. Rev. B*, **48**, 10917 (1993).
19. F. Maier, M. Riedel, B. Mantel, J. Ristein, and L. Ley, *Phys. Rev. Lett.*, **85**, 3472 (2000).
20. M. Riedel, J. Ristein, and L. Ley, *Phys. Rev. B*, **69**, 125338 (2004).
21. J. Angus, Private communication.
22. V. Chakrapani, S. C. Eaton, and J. Angus, Abstract 519, The Electrochemical Society Meeting Abstracts, Vol. 2003-01, Paris, France, April 27-May 2, 2003.
23. G. Piantanida, A. Breskin, R. Chenik, O. Katz, A. Laikhtman, A. Hoffman, and C. Coluzza, *J. Appl. Phys.*, **89**, 8259 (2001).